

**Viscous fingering in a horizontal flow through a porous medium induced by chemical reactions under isothermal and adiabatic conditions**

Subramanian Swernath and S. Pushpavanam

Citation: *The Journal of Chemical Physics* **127**, 204701 (2007); doi: 10.1063/1.2799999

View online: <http://dx.doi.org/10.1063/1.2799999>

View Table of Contents: <http://scitation.aip.org/content/aip/journal/jcp/127/20?ver=pdfcov>

Published by the [AIP Publishing](#)

---

**Articles you may be interested in**

[Linear stability analysis of Korteweg stresses effect on miscible viscous fingering in porous media](#)

*Phys. Fluids* **25**, 074104 (2013); 10.1063/1.4813403

[Miscible viscous fingering with linear adsorption on the porous matrix](#)

*Phys. Fluids* **19**, 073101 (2007); 10.1063/1.2743610

[Viscous fingering of miscible slices](#)

*Phys. Fluids* **17**, 054114 (2005); 10.1063/1.1909188

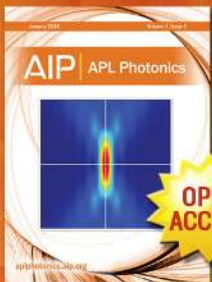
[Nonlinear interactions of chemical reactions and viscous fingering in porous media](#)

*Phys. Fluids* **11**, 949 (1999); 10.1063/1.869988

[A numerical study of chemical front propagation in a Hele-Shaw flow under buoyancy effects](#)

*Phys. Fluids* **10**, 775 (1998); 10.1063/1.869602

---



**Launching in 2016!**  
The future of applied photonics research is here

**OPEN ACCESS**

**AIP** | APL  
Photonics

# Viscous fingering in a horizontal flow through a porous medium induced by chemical reactions under isothermal and adiabatic conditions

Subramanian Swernath and S. Pushpavanam<sup>a)</sup>

Department of Chemical Engineering, I. I. T. Madras, Tamilnadu, Chennai 600 036, India

(Received 9 July 2007; accepted 26 September 2007; published online 26 November 2007)

In this work we analyze the viscous fingering instability induced by an autocatalytic chemical reaction in a liquid flowing horizontally through a porous medium. We have analyzed the behavior of the system for isothermal as well as adiabatic conditions. The kinetics of the reaction is chosen so that the rate depends on the concentration of only a single species. Since the reaction is autocatalytic the system admits a traveling wave solution. For endothermic reactions the concentration wave and temperature wave are mirror images, whereas for an exothermic reaction they are similar or parallel. The viscosity of the fluid is assumed to depend strongly on the concentration of the product and temperature of the medium. The dependence of viscosity on concentration (decrease with concentration) can destabilize the traveling wave resulting in the formation of viscous fingers. We have performed a linear stability analysis to determine the stability of the base traveling wave solution. The stability predictions have been confirmed by nonlinear simulations of the governing equations based on a finite difference scheme. We observe that including the temperature dependency of viscosity stabilizes the flow for an endothermic reaction, i.e., regions which exhibited viscous fingering now demonstrate stable displacement. For exothermic systems, however, the system exhibits less stable behavior under adiabatic conditions, i.e., it is destabilized by both concentration and temperature dependencies of viscosity. © 2007 American Institute of Physics. [DOI: 10.1063/1.2799999]

## I. INTRODUCTION

Fluid displacement processes in porous media have been investigated extensively as they have wide applications in various chemical and petroleum industries, chromatographic separation, fixed bed regeneration, etc. Here one fluid displaces another fluid which is already occupying the porous medium. The two fluids may be miscible or immiscible. The differences in the density and/or viscosity of the fluids determine the flow behavior in the porous bed. The shape of the interface between the fluids is determined by these properties. The displacement of one fluid by another as a plug may get disturbed even in a homogeneous porous medium if a low viscous fluid displaces a high viscous fluid. Hence, the dynamics of such flow systems with a special emphasis on stability of flows as determined by the interface must be understood. Chemohydrodynamic interactions arise when chemical reactions are also present in these systems. Here there is a chemical reaction which can affect the flow especially if the fluid properties such as viscosity depend on the concentration of the various species.

We now give insight into the physical basis of this instability. Consider the process in which a low viscous fluid invades and displaces a porous medium filled with a high viscous fluid. Consider a disturbance to the interface between the two fluids which is initially flat. This can get amplified giving rise to fingers developing along the interface. This

phenomenon is called viscous fingering. The system is schematically shown in Fig. 1. When the interface is flat, the effective viscosity across the medium does not vary with  $y$ . Consider the interface deformed as shown in Fig. 1 so that in the middle it is deflected to the right. In such a situation the effective viscosity in the middle is lower as the low viscosity fluid on the left occupies a larger length. As the total pressure drop is a constant across the medium, the flow is higher in the middle and the instability gets amplified. It can be established using similar arguments that, when a more viscous fluid displaces a less viscous fluid, the interface shape remains flat, i.e., the disturbances of the interface shape decay.<sup>1,2</sup> This problem has been extensively investigated in the literature. One of the early investigations was carried by Hill<sup>3</sup> who studied the problem in the context of sugar sweetening off (extraction) process. His work was a purely experimental study. Peaceman and Rachford<sup>4</sup> carried out a numerical simulation of the miscible displacement of two fluids. They used a finite difference method for discretizing the partial differential equations governing the fluid flow. They then

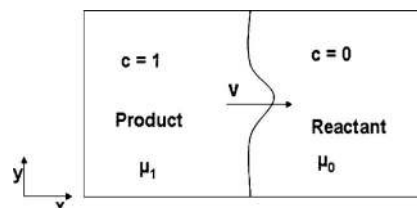


FIG. 1. Schematic of the system under study.

<sup>a)</sup>Electronic mail: spush@iitm.ac.in

used a leapfrog approach for solving the equations numerically. The grids chosen were, however, very coarse. The numerical algorithm involved obtaining the solution directly in terms of pressure and velocity instead of using a stream function and vorticity formulation. The work was further extended by Christie and Bond<sup>5</sup> (incorporating diffusion, grid refinement, etc.) where they calculate the linear stability and compares with their nonlinear predictions. The experimental match was also obtained with a previously published article. Tan and Homsy<sup>6</sup> studied the stability of miscible fluid flow. They analyzed the situation where a low viscous fluid displaces a high viscosity fluid. The viscosity of the fluid was determined by the concentration of a nonreactive species. They used a quasi-steady-state approximation (QSSA) as the concentration profile in the base state was time dependent. The results based on QSSA were compared with those based on simulations for several initial conditions to study the effect of the approximation. In a later study, Tan and Homsy<sup>7</sup> analyzed the nonlinear behavior of viscous fingering in a porous media. The numerical algorithm was based on a Fourier spectral method. They studied the behavior of the system using two dimensionless groups Peclet number (Pe) and mobility ratio  $M$  (ratio of viscosity of the two fluids). However, there were no chemical reactions in the system studied. There was a good agreement of the predictions of this work with that of the previous work<sup>6</sup> particularly in the initial stages of the disturbance development. However, at later time instants, they observed some new phenomena generated by the nonlinear interactions in the system which were not captured by the linear stability theory. Homsy<sup>1</sup> discusses and compares the similarities and differences of the instability in the case of miscible and immiscible displacements. De Wit and Homsy<sup>8,9</sup> analyzed the coupling between viscous fingering and chemical reactions in horizontal flows. They used a kinetic expression which admits two stable steady states and an unstable one. They discussed directly the results of the nonlinear simulations describing the behavior of the system. In particular, the linear stability analysis of this system was not carried out. This kinetics shows droplet formation of the invading fluid in the nonlinear simulation. This phenomenon was also observed in the vertical configuration when the flow was driven by a density gradient.<sup>10</sup> This was explained on the basis of the presence of two stable steady states. De Wit<sup>11</sup> used similar kinetics and analyzed the stability of a chemohydrodynamic system in a vertical configuration (induced by density differences with a constant viscosity) using the traveling front as a base state. Isothermal traveling waves have been determined analytically, and the expressions for these waves is given in the book by Murray.<sup>12</sup> The stability of the traveling wave of chemical concentration in a reactive flow obtained from a linear analysis results in dispersion curves which are time independent.<sup>11</sup> Linear stability analysis of these systems has been carried out along the lines of Yang *et al.*<sup>13</sup> The temperature effects on a vertically aligned system with a constant viscosity and variable density were studied by Kalliadasis *et al.*<sup>14</sup> for an exothermic reaction. They considered the case when the effects of concentration and temperature on density oppose each other. An extension of this work incorporating the effect of heat losses was carried out

by D'Heroncourt *et al.*,<sup>15</sup> where they found that in the presence of heat losses the traveling wave is converted to pulses. The viscous fingering instabilities due to the combined effect of temperature and concentration in a radial Hele-Shaw cell has been studied for horizontal flows by Pritchard.<sup>16</sup> He analyzed a nonreactive flow situation and carried out a linear stability analysis of the system. There was no observation of stabilization of an unstable thermal front by the compositional front. Experimental work has been carried out using a single fluid exploiting the temperature gradients to generate viscosity differences.<sup>17,18</sup> The results of their experiments have been verified with numerical simulations. The thermal front is usually more diffusive than the concentration front. These authors, hence, found that a high viscosity contrast and a high inlet velocity are required for the interface to deform. Concentration gradients were absent as they had used glycerine of uniform composition in their work.

Most of the work in the literature to date in this context has focused on analyzing the behavior of systems when viscosity is only a function of concentration for horizontal flows. In this work we assume that the viscosity strongly depends on concentration as well as temperature prevailing in the flow domain. The linear stability analysis is carried out using the approach proposed in De Wit.<sup>11</sup> We obtain critical conditions about which the stability of the traveling wave changes. We study adiabatic systems sustaining exothermic as well as endothermic reactions to determine conditions when the concentration and temperature dependency of viscosity influence the stability in tandem or counteract. The reaction kinetics is assumed to be of the form followed by iodate-arsenous acid (IAA) reaction. A one variable model representing the evolution of iodide concentration was found to be sufficient to describe the reaction.<sup>19</sup> In the vertical configuration, where density is a function of concentration, there have been several earlier studies in both the numerical as well as the experimental analysis specifically relating to the fingering dynamics of IAA reaction.<sup>20,21</sup> In these early studies in the literature, the combined effect of concentration and temperature dependence of viscosity (horizontal) has not been investigated in reacting systems. So here we carry out an analysis of an adiabatic system sustaining chemical reactions with significant heat effects and analyze the onset of viscous fingering through linear stability analysis and nonlinear simulations. Linear stability predictions are verified using nonlinear simulations by varying the dimensionless parameters  $Da$ ,  $R_c$ ,  $R_T$ , Pe, and Le.  $R_c$  is the dimensionless parameter which measures viscosity or mobility dependence as a function of concentration and  $R_T$  defines the temperature dependent component of viscosity.

The paper is organized as follows. In Sec. II we formulate the model equations in nondimensional form incorporating the viscosity dependency on both concentration and temperature. In Sec. III, we discuss the evolution of the traveling front and the base state for various situations. In Sec. IV the emphasis is on the linear stability of the traveling front where viscosity is a function of concentration and/or temperature. In Sec. V we discuss the nonlinear behavior of the

system. Different flow patterns are analyzed and the effect of various parameters is studied to validate the predictions of the linear stability analysis.

## II. MODEL

We consider a homogeneous 2D porous medium of length  $L$  (along  $x$ ) and width  $H$  (along  $y$ ) with a constant permeability  $K$  (Fig. 1). An incompressible liquid containing a solute is injected from the left with a uniform velocity  $U$  along the  $x$  direction. The solute initiates an autocatalytic reaction, and the rate of product formation is described by a rate expression which is representative of the IAA reaction.<sup>15</sup> The evolution of the system is governed by the laws of conservation of mass, momentum, and energy. We first discuss the equations which govern the flow under adiabatic conditions. The superscript  $*$  is used to indicate variables with dimensions.

### A. Adiabatic case

The equation of continuity is given by

$$\nabla^* \cdot \mathbf{u}^* = 0. \quad (1)$$

The pressure distribution in the porous medium is obtained from Darcy's law,

$$\nabla^* P^* = -\frac{\mu}{K} \mathbf{u}^*. \quad (2)$$

The evolution of the product species concentration is given by

$$\frac{\partial c^*}{\partial t^*} + \mathbf{u}^* \cdot \nabla^* c^* = D \nabla^{*2} c^* + f(c^*). \quad (3)$$

The evolution of temperature  $T^*$  is governed by

$$\rho c_p \left[ \frac{\partial T^*}{\partial t^*} + \mathbf{u}^* \cdot \nabla^* T^* \right] = \kappa \nabla^{*2} T^* + (-\Delta H) f(c^*). \quad (4)$$

The rate expression for the reaction is given by  $f(c^*) = -c^*(k_a + k_r c^*)(c^* - c_0^*)$ . Here,  $k_a = k_1 [H^+]^2$  and  $k_r = k_2 [H^+]^2$ , where  $k_1$  and  $k_2$  are rate constants. In these equations,  $\nabla^*$  signifies that the independent variables are  $x^*$  and  $y^*$ . We rewrite these equations in a frame of reference which moves with a velocity  $U$ . We have in this frame

$$x_m^* = x^* - Ut, \quad (5)$$

$$u_m^* = u^* - U. \quad (6)$$

We do not have any characteristic length or time scales which arise spontaneously for an infinitely long system. We define the nondimensional variables using the scales

$$P_{\text{ch}} = \frac{\mu D}{K},$$

$$t_{\text{ch}} = \frac{D}{U^2},$$

$$x_{\text{ch}} = \frac{D}{U}, \quad (7)$$

$$u_{\text{ch}} = U,$$

$$c_{\text{ch}} = c_0^*,$$

$$T_{\text{ch}} = T_0 \phi.$$

Here,  $T_0$  and  $c_0^*$  represent the temperature and the concentration of the product at the inlet (left face) to the system. Here,  $\phi = [(-\Delta H) c_0 / \rho_0 c_p T_0]$  represents a dimensionless heat of reaction parameter. The dimensionless temperature  $T$  is defined as  $(T^* - T_0) / T_0 \phi$ .

The equations are nondimensionalized in the moving reference frame using these scales. The corresponding dimensionless equations can then be written as

$$\frac{\partial u}{\partial x} + \frac{\partial w}{\partial y} = 0, \quad (8)$$

$$\frac{\partial P}{\partial x} = -\mu(u + 1), \quad (9)$$

$$\frac{\partial P}{\partial y} = -\mu w, \quad (10)$$

$$\frac{\partial c}{\partial t} + u \frac{\partial c}{\partial x} + w \frac{\partial c}{\partial y} = \frac{\partial^2 c}{\partial x^2} + \frac{\partial^2 c}{\partial y^2} + \text{Daf}(c). \quad (11)$$

The energy equation becomes

$$\frac{\partial T}{\partial t} + u \frac{\partial T}{\partial x} + w \frac{\partial T}{\partial y} = \text{Le} \left[ \frac{\partial^2 T}{\partial x^2} + \frac{\partial^2 T}{\partial y^2} \right] + \text{sgn}(\phi) \text{Daf}(c). \quad (12)$$

In the above two equations  $f(c) = -c(c-1)(c+d)$ . The parameter “ $d$ ” arising in the kinetic expression can be defined as  $d = k_a / k_r c_0$ . Here,  $\text{Le} = D_T / D_c$  is the ratio of thermal diffusivity to mass diffusivity, and  $\text{sgn}(\phi) = 1$  for exothermic reactions and  $\text{sgn}(\phi) = -1$  for endothermic reactions.  $\tau_H = D / U^2$  is the hydrodynamic time scale, where the reaction time scale is  $\tau_c = 1 / k_r c_0^2$ . Damkohler number represents the ratio of hydrodynamic to chemical time scales and can be represented as  $\text{Da} = \tau_H / \tau_c = D k_r c_0^2 / U^2$ . Pe determines the ratio of rate of convective transport to the rate of diffusive transport and is represented mathematically as  $\text{Pe} = UL / D$ . Pe represents the dimensionless width of the domain.

We assume the viscosity of the fluid to vary with concentration and temperature as

$$\mu = \mu_0 e^{[-R_c c + R_T T]}. \quad (13)$$

This results in

$$\frac{1}{\mu} \frac{d\mu}{dc} = -R_c, \quad (14)$$

$$\frac{1}{\mu} \frac{d\mu}{dT} = R_T.$$

From Eq. (14) we observe that an instability due to composition arises when  $R_c > 0$ , and an instability due to temperature would arise when  $R_T < 0$  for an exothermic reaction and  $R_T > 0$  for an endothermic reaction as will be seen later. We consider only liquid phase systems and restrict ourselves to  $R_T < 0$ . Equations (8)–(12) are converted in terms of stream function and vorticity ( $\psi$ - $\omega$ ) by defining  $u = \partial\psi/\partial y$  and  $w = -\partial\psi/\partial x$ . We evaluate the curl of the momentum equation and obtain

$$\nabla^2 \psi = -\omega, \quad (15)$$

$$\omega = -R_c \left( \frac{\partial\psi}{\partial x} \frac{\partial c}{\partial x} + \frac{\partial\psi}{\partial y} \frac{\partial c}{\partial y} + \frac{\partial c}{\partial y} \right) + R_T \left( \frac{\partial\psi}{\partial x} \frac{\partial T}{\partial x} + \frac{\partial\psi}{\partial y} \frac{\partial T}{\partial y} + \frac{\partial T}{\partial y} \right), \quad (16)$$

$$\frac{\partial c}{\partial t} + \frac{\partial\psi}{\partial y} \frac{\partial c}{\partial x} - \frac{\partial\psi}{\partial x} \frac{\partial c}{\partial y} = \nabla^2 c + \text{Daf}(c), \quad (17)$$

$$\frac{\partial T}{\partial t} + \frac{\partial\psi}{\partial y} \frac{\partial T}{\partial x} - \frac{\partial\psi}{\partial x} \frac{\partial T}{\partial y} = \text{Le} \nabla^2 T + \text{sgn}(\phi) \text{Daf}(c). \quad (18)$$

We use periodic boundary conditions for concentration and temperature along the  $y$  direction ( $[y=0, y=Pe]$  the direction transverse to the flow). This is tantamount to seeking a solution which extends periodically in the transverse direction. This enables us to eliminate end effects along that direction. Along the  $x$  (axial) direction, we impose Dirichlet boundary condition where we use  $c=1$  at the left boundary ( $x=0$ ) and  $c=0$  at the right boundary ( $x=APe$ ) (Fig. 1). Here, the products are fed on the left boundary to initiate the autocatalytic reaction in the porous medium containing the reactant and the front moves from left to right. The boundary conditions of dimensionless temperature are  $T(x=0)=1$  and  $T(x=APe)=0$  for an exothermic reaction. For endothermic reactions, the temperature boundary conditions get inverted along the  $x$  direction and we use  $T(x=0)=0$  and  $T(x=APe)=1$ . No boundary conditions are required for the vorticity as it is defined by an algebraic expression.  $\psi=0$  is applied at the boundaries along the  $x$  direction ( $x=0$  and  $x=APe$ ) as there is no net flow across the surfaces in a moving reference frame. Along the transverse direction, we incorporate periodic boundary conditions. These can be represented mathematically as  $\psi(y=0)=\psi(y=Pe)$  and  $d\psi/dy|_{y=0}=d\psi/dy|_{y=Pe}$ .<sup>22,23</sup> Since the reaction is autocatalytic, the interface keeps moving from left to right at a velocity determined by the reaction kinetics. This is the velocity with respect to a moving reference frame. It represents a constant velocity with respect to  $U$ , with which the reaction front moves in the system.

## B. Isothermal

For this case the system temperature is a constant and the temperature dependency on viscosity can be neglected. Now, the viscosity variation is of the form  $\mu = \mu_0 e^{-R_c c}$ . It is equivalent to setting  $R_T$  as zero in Eq. (13). Hence, the set of equations to be solved becomes Eqs. (8)–(11). The energy balance governed by Eq. (12) to determine the temperature is eliminated. These equations are converted to the stream function-vorticity forms as described earlier. We obtain the set of equations [Eqs. (15)–(17)] which describes the system behavior now.

## III. TRAVELING FRONTS

The system of equations described by Eqs. (8)–(12) admits a base state solution in the form of a traveling wave. This arises as the system admits two spatially uniform steady states. “ $c=1$ ” is the stable chemical steady state of the cubic kinetics corresponding to the products of the reaction, and “ $c=0$ ” is the unstable state corresponding to the reactants.<sup>15</sup> This is generated by the nonlinear interactions between kinetics and diffusion. The traveling wave is the trajectory connecting the two steady states. This state corresponds to the situation where there is no convection ( $u=0$ ). For the traveling front, we seek a solution where the variables depend only on a single variable  $z$  given by  $z=x-vt$ . Here,  $v$  is the traveling wave velocity and is given by  $v=(\sqrt{\text{Da}/2})(1+2d)$ .<sup>11</sup> The wave generated is one dimensional (i.e., it travels in the  $x$ -direction). In the moving reference frame for an isothermal system, the traveling front is a chemical concentration wave, which arises due to the propagation of the reaction front. There is no bulk motion or convection in the moving reference frame. As the velocity component of the convective-diffusion equation is zero, the equations governing the evolution of the traveling front become

$$-v \frac{dc_{ss}}{dz} = \frac{d^2 c_{ss}}{dz^2} + \text{Daf}(c_{ss}), \quad (19)$$

$$-v \frac{dT_{ss}}{dz} = \text{Le} \frac{d^2 T_{ss}}{dz^2} + \text{sgn}(\phi) \text{Daf}(c_{ss}). \quad (20)$$

In an infinite domain [Eq. (19)] the base state traveling wave solution for an isothermal system is

$$c(x,t) = \frac{1}{1 + e^{-(\sqrt{\text{Da}/2})(x-vt)}}. \quad (21)$$

For the exothermic reaction situation when  $\text{Le}=1$ , we have  $T(x,t)=c(x,t)$ . Here the traveling front can be calculated analytically for both variables as the analytical solution for Eq. (19) already exists. The same solution applies to Eq. (20) for a situation where the thermal diffusivity is the same as concentration diffusivity for  $\text{Le}=1$ . For other conditions where  $\text{Le} \neq 1$ , the base state solution has to be obtained numerically and on a finite domain. For this, the two second order equations [Eqs. (19) and (20)] are converted to four first order equations. The two point boundary value problem is solved numerically using a fourth order Runge-Kutta scheme employing a shooting method. The domain is chosen

to extend from  $z=-z_1$  to  $z=z_1$ . The numerical method converges for sufficiently large  $z_1$ . The independence of the solution to the choice of  $z_1$  was established. The boundary conditions which the traveling wave satisfies for the two reactions are as given below.

- Exothermic reaction,

$$z = -z_1, \quad c_{ss} = 1, \quad T_{ss} = 1, \quad (22)$$

$$z = z_1, \quad c_{ss} = 0, \quad T_{ss} = 0.$$

- Endothermic reaction,

$$z = -z_1, \quad c_{ss} = 1, \quad T_{ss} = 0, \quad (23)$$

$$z = z_1, \quad c_{ss} = 0, \quad T_{ss} = 1.$$

For an isothermal system, the temperature variation is zero and we do not solve for the temperature profile. Only the concentration equation needs to be solved with the corresponding boundary conditions for the traveling wave.

The domain size required for convergence varies with  $Le$  and  $Da$ . This is because an increase in  $Da$  leads to sharper fronts and so the total domain size for convergence gets reduced significantly. For each parameter set, the domain independency of the numerically obtained traveling wave is verified before the linear stability calculations are carried out. For an isothermal system only the concentration front is generated. The variation of both concentration and temperature is from 1 to 0 for an exothermic reaction as we move from left to right [Fig. 2(a)]. In the case of an exothermic reaction, the concentration and temperature wave coincide with each other for  $Le=1$ . In the figure we also depict the analytical solution obtained when the domain is infinitely long. It can be seen that our numerical solution for concentration for a finite domain agrees closely with the analytical solution for an infinite domain. For  $Le>1$ , the heat diffusion is faster than concentration diffusion and the thermal wave front exhibits a more diffusive behavior (less sharp front). The nature of temperature wave for  $Le=5$  is also shown in Fig. 2(a). The concentration wave remains the same for all  $Le$ . This is because the  $Le$  affects only the equation governing the temperature. The thermal front is a smoothly varying curve for a very high  $Le$  showing the dominance of thermal diffusion. The variation of the concentration is from 1 to 0 but that of temperature is from 0 to 1 as we move from left to right for an endothermic reaction. Figure 2(b) depicts the shape of the concentration and thermal front for the traveling wave for an endothermic reaction with  $Le=1$ . The concentration and temperature waves are mirror images to each other. There would be a significant difference in these fronts for a  $Le$  other than 1. This reflective symmetry is destroyed when  $Le$  attains a value other than unity.

## IV. LINEAR STABILITY

### A. Nonisothermal system

An instability in the traveling wave results in the phenomenon of viscous fingering. This section describes the al-

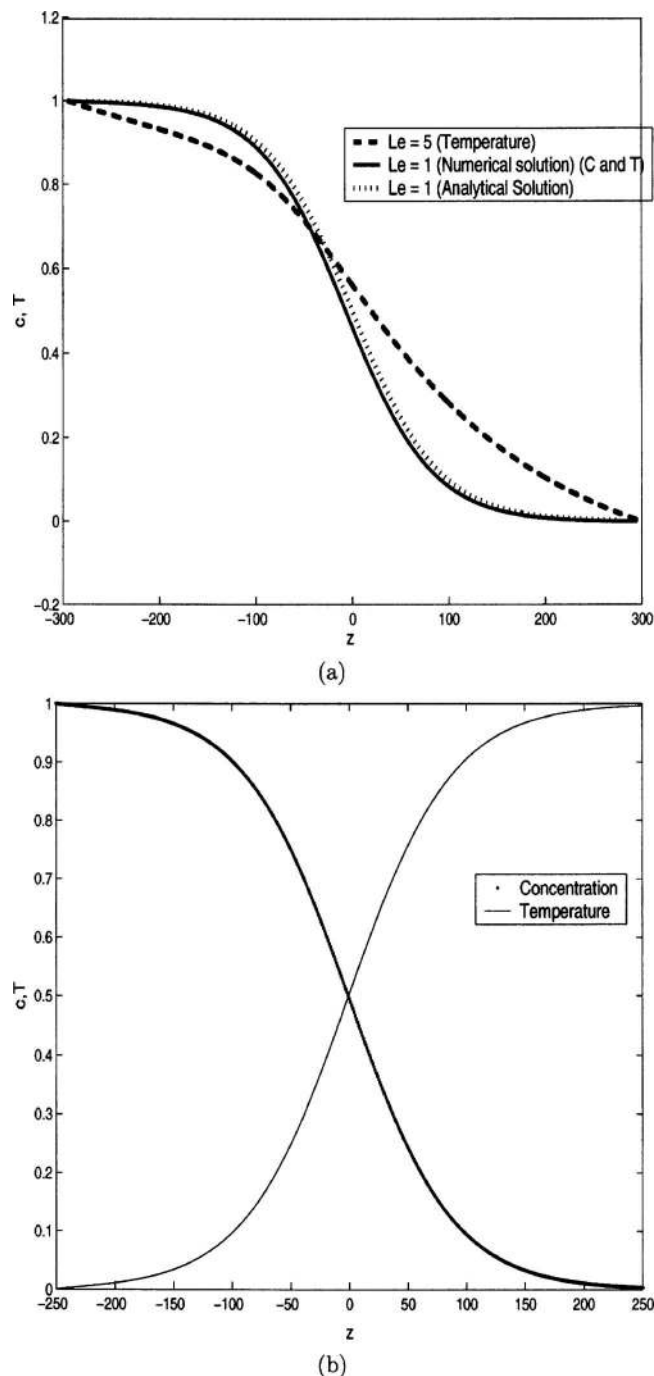


FIG. 2. Traveling wave fronts for (a) exothermic and (b) endothermic reaction for  $Da=0.001$ ,  $d=0.1$ , and varying  $Le$ .

gorithm used to determine the conditions at which the interface becomes unstable. To determine the stability of the traveling wave solution a perturbation is given to the variables and we study how this evolves with time. The base state is the traveling wave, which is described as

$$u_{ss} = 0, \quad w_{ss} = 0, \quad c = c_{ss}(z), \quad P = P_{ss}(z), \quad T = T_{ss}(z).$$

The perturbation variables or deviations from the traveling wave solution are defined as

$$\begin{aligned}\tilde{c} &= c - c_{ss}(z), \\ \tilde{P} &= P - P_{ss}(z), \\ \tilde{T} &= T - T_{ss}(z), \\ \tilde{w} &= w - w_{ss}, \\ \tilde{u} &= u - u_{ss}.\end{aligned}\quad (24)$$

The terms with  $\sim$  represent the perturbations from the base state. The governing equations of the base state can be represented as

$$\frac{\partial u_{ss}}{\partial z} + \frac{\partial w_{ss}}{\partial y} = 0, \quad (25)$$

$$\frac{\partial P_{ss}}{\partial z} = -\mu_{ss}(u_{ss} + 1), \quad (26)$$

$$\frac{\partial P_{ss}}{\partial y} = -\mu_{ss}w_{ss}, \quad (27)$$

$$-v \frac{\partial c_{ss}}{\partial z} + u_{ss} \frac{\partial c_{ss}}{\partial z} + w_{ss} \frac{\partial c_{ss}}{\partial y} = \frac{\partial^2 c_{ss}}{\partial z^2} + \frac{\partial^2 c_{ss}}{\partial y^2} + \text{Daf}(c_{ss}), \quad (28)$$

$$-v \frac{\partial T_{ss}}{\partial z} + u_{ss} \frac{\partial T_{ss}}{\partial z} + w_{ss} \frac{\partial T_{ss}}{\partial y} = \text{Le} \left[ \frac{\partial^2 T_{ss}}{\partial z^2} + \frac{\partial^2 T_{ss}}{\partial y^2} \right] + \text{sgn}(\phi) \text{Daf}(c_{ss}). \quad (29)$$

The viscosity of the base state  $\mu_{ss}$  depends on “z,” since it varies with concentration and temperature which are functions of “z.” Linearizing Eqs. (8)–(12) around the above steady state, we have

$$\frac{\partial \tilde{u}}{\partial z} + \frac{\partial \tilde{w}}{\partial y} = 0, \quad (30)$$

$$\frac{\partial \tilde{P}}{\partial z} = -\mu_{ss} \tilde{u} - \left. \frac{\partial \mu}{\partial c} \right|_{ss} \tilde{c} - \left. \frac{\partial \mu}{\partial T} \right|_{ss} \tilde{T}, \quad (31)$$

$$\frac{\partial \tilde{P}}{\partial y} = -\mu_{ss} \tilde{w}, \quad (32)$$

$$\frac{\partial \tilde{c}}{\partial t} - v \frac{\partial \tilde{c}}{\partial z} + \tilde{u} \frac{\partial c_{ss}}{\partial z} = \frac{\partial^2 \tilde{c}}{\partial z^2} + \frac{\partial^2 \tilde{c}}{\partial y^2} + \text{Da} \left. \frac{\partial f}{\partial c} \right|_{ss} \tilde{c}, \quad (33)$$

$$\begin{aligned}\frac{\partial \tilde{T}}{\partial t} - v \frac{\partial \tilde{T}}{\partial z} + \tilde{u} \frac{\partial T_{ss}}{\partial z} \\ = \text{Le} \left[ \frac{\partial^2 \tilde{T}}{\partial z^2} + \frac{\partial^2 \tilde{T}}{\partial y^2} \right] + \text{sgn}(\phi) \text{Da} \left. \frac{\partial f}{\partial c} \right|_{ss} \tilde{c}.\end{aligned}\quad (34)$$

We seek the solution for the deviation variables in the form of

$$\begin{aligned}\tilde{c} &= \bar{c} e^{\sigma t} e^{iky}, \\ \tilde{u} &= \bar{u} e^{\sigma t} e^{iky}, \\ \tilde{w} &= \bar{w} e^{\sigma t} e^{iky}, \\ \tilde{P} &= \bar{P} e^{\sigma t} e^{iky}, \\ \tilde{T} &= \bar{T} e^{\sigma t} e^{iky}.\end{aligned}\quad (35)$$

Here,  $\sigma$  is the growth constant and  $k$  represents the wave number.  $\sigma$  determines how fast the perturbation evolves with time, whereas  $k$  represents the spatial frequency along the transverse (y) direction at the instant the finger formation is initiated. Equations (36)–(38) are solved simultaneously along with the base state solution. We eliminate  $\bar{w}$  and  $\bar{P}$  from Eqs. (30)–(34) and obtain the equations describing  $\bar{u}$ ,  $\bar{c}$ , and  $\bar{T}$ . This results in the set of the following three equations with three unknowns:

$$\frac{d^2 \bar{u}}{dz^2} + \left[ -R_c \frac{dc_{ss}}{dz} + R_T \frac{dT_{ss}}{dz} \right] \frac{d\bar{u}}{dz} - k^2 \bar{u} + k^2 R_c \bar{c} - k^2 R_T \bar{T} = 0, \quad (36)$$

$$\frac{d^2 \bar{c}}{dz^2} - k^2 \bar{c} + v \frac{d\bar{c}}{dz} - \bar{u} \frac{dc_{ss}}{dz} + \text{Da} \frac{\partial f}{\partial c} \bar{c} = \sigma \bar{c}, \quad (37)$$

$$\text{Le} \left[ \frac{d^2 \bar{T}}{dz^2} - k^2 \bar{T} \right] + v \frac{d\bar{T}}{dz} - \bar{u} \frac{dT_{ss}}{dz} + \text{sgn}(\phi) \text{Da} \frac{\partial f}{\partial c} \bar{c} = \sigma \bar{T}. \quad (38)$$

The above set of equations [Eqs. (36)–(38)] is discretized using a second order finite difference scheme and solved. They are written in the generalized matrix form as  $\mathbf{Ax} = \sigma \mathbf{Bx}$ ,

$$(A) \begin{pmatrix} \bar{u} \\ \bar{c} \\ \bar{T} \end{pmatrix} = \sigma \begin{pmatrix} 0 & 0 & 0 \\ 0 & 1 & 0 \\ 0 & 0 & 1 \end{pmatrix} \begin{pmatrix} \bar{u} \\ \bar{c} \\ \bar{T} \end{pmatrix}. \quad (39)$$

The elements of the matrix  $\mathbf{A}$  are

$$\begin{aligned}A_{11} &= \left[ \frac{d^2}{dz^2} + \left[ -R_c \frac{dc_{ss}}{dz} + R_T \frac{dT_{ss}}{dz} \right] \frac{d}{dz} - k^2 \right], \\ A_{12} &= k^2 R_c, \quad A_{13} = -k^2 R_T, \\ A_{21} &= -\frac{dc_{ss}}{dz}, \\ A_{22} &= \left[ \frac{d^2}{dz^2} - k^2 + v \frac{d}{dz} + \text{Da} \frac{\partial f}{\partial c} \right], \quad A_{23} = 0, \\ A_{31} &= -\frac{dT_{ss}}{dz}, \quad A_{32} = +\text{sgn}(\phi) \text{Da} \frac{\partial f}{\partial c},\end{aligned}\quad (40)$$

$$A_{33} = \left[ \text{Le} \left[ \frac{d^2}{dz^2} - k^2 \right] + v \frac{d}{dz} \right].$$

The values of  $c_{ss}$ ,  $T_{ss}$ ,  $dc_{ss}/dz$ , and  $dT_{ss}/dz$  are required in the above matrix coefficients. Consequently, these values of the traveling wave solution are obtained at the discrete points and are used for determining the stability. The maximum eigenvalue corresponding to each wave number is plotted for a fixed set of dimensionless parameters and this yields the dispersion curve. This curve is used to determine the stability of the flow as will be explained later.

The system here admits a traveling wave solution because of the choice of specific autocatalytic reaction kinetics which admits two possible steady states. The dispersion curve now is invariant with time due to the existence of the traveling wave between the two steady states. This is the primary difference from the situation prevailing in a horizontal flow without reaction which has been analyzed by Tan and Homsy.<sup>6</sup> For the case without the reaction the growth rate as well as the base state concentration and temperature profiles are functions of time and can be approximated by an error function as shown by Tan and Homsy.<sup>6</sup> A QSSA is necessary to analyze the situation of the nonreactive flow.

## B. Isothermal case

For the isothermal situation the temperature is a constant. We use  $R_T=0$  in Eq. (36) and do not include Eq. (38) in the stability calculations. The matrix equations determining the stability reduces to

$$(A) \begin{pmatrix} \bar{u} \\ \bar{c} \end{pmatrix} = \sigma \begin{pmatrix} 0 & 0 \\ 0 & 1 \end{pmatrix} \begin{pmatrix} \bar{u} \\ \bar{c} \end{pmatrix}. \quad (41)$$

The linear stability analysis helps us to determine the conditions when there is a qualitative change in the velocity field from that prevailing in the traveling wave solution. In the traveling wave, there is concentration and temperature varying along “z” alone with no bulk convective flow. The other state the system can exhibit is one where the velocity field varies spatially and temporally. This results in a concentration field which varies spatially in two dimensions. The characteristic feature of this is there is no sharp interface which separates the two fluids and the concentration and velocity also vary in the direction normal to the flow. The results of the linear stability calculations help us determine when this transition in behavior occurs. These are depicted in the form of dispersion curves. These are the curves which show the dependency of the maximum growth constant on wave number. When the dispersion curve is such that the maximum  $\sigma$  is negative for all wave numbers, we conclude that the system is stable and no fingers are formed. If the growth exhibits a positive maximum for a particular range of wave numbers, the system is unstable and the system exhibits a spatial periodicity with this wave number at the onset of instability.

We first discuss the dispersion curves for the isothermal system. Here, the temperature is constant and only  $R_c$  determines the system stability. Figure 3(a) shows the dispersion curves for three different values of  $R_c$ . It is seen that, as the

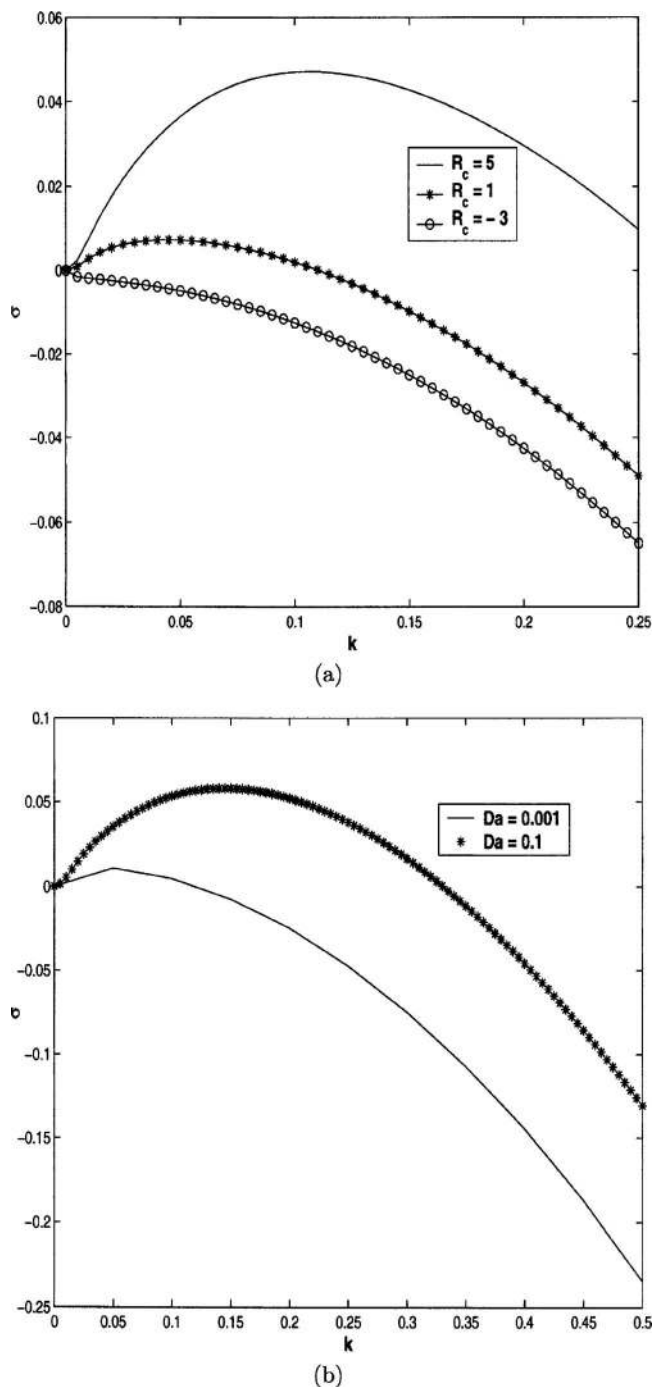


FIG. 3. Dispersion curve showing the variation of growth constant with wave number. (a) Effect of  $R_c$  for an isothermal reaction for  $Da=0.01$  and  $d=0.1$ . (b) Effect of  $Da$  for an isothermal reaction for  $R_c=3$ ,  $d=0.1$ .

mobility ratio increases from a negative to a positive value, the dispersion curve moves upwards. The growth rate is positive for a band of wave numbers as soon as  $R_c > 0$ . Under these conditions ( $R_c > 0$ ) the low viscous fluid invades a high viscous fluid leading to the fingered interface. The traveling front which is independent of the transverse direction gets deformed and it exhibits a periodicity in that direction. This periodicity is determined by the critical wave number at which the growth rate is maximum. The dispersion curves confirm that the system instability is pronounced at large positive mobility ratios. A positive mobility ratio corre-

sponds to a less viscous fluid displacing a high viscous fluid. Consider a disturbance that deforms an interface and generates a finger. The effective viscosity is lower where a finger is present. Hence, there is a larger tendency for the fingers to move ahead of the average front. This leads to faster moving fingers and, hence, they become longer and they persist. If the mobility ratios are negative, the traveling front is always found to be stable. This is due to the fact that here a higher viscosity fluid invades a lower viscosity fluid and, thus, a favorable situation prevails for the fluid to move as a plug. The critical wave number where the growth rate is a maximum is seen to shift towards a larger value as we increase  $R_c$ . So the number of fingers also increases with an increase in mobility ratio. Figure 3(b) shows the effect of  $Da$  on the finger formation for  $R_c=3$  and  $d=0.1$ . The increase in  $Da$  results in the system becoming more unstable as can be seen by the dispersion curve moving upwards. Reactive fingers are thus more unstable than their nonreactive counterparts. A lower  $Da$  implies a smaller effect of reaction and a more dominant effect of diffusion. The chemical front becomes sharper as reaction terms dominate the flow at high  $Da$ , whereas at low  $Da$  the diffusion terms dominate the flow. Consequently, the viscosity and the concentration gradients are steeper for the higher  $Da$  values and this makes the system more prone to instability. An increase in  $Da$  results in a shift of the critical wave number towards the right. Thus, the number of fingers is increased or the wavelength of the finger is reduced as  $Da$  increases. We have also studied the effect of the kinetic parameter  $d$  on the stability of flow for  $R_c=3$  and  $Da=0.01$ . This parameter cannot be changed easily once the reaction is fixed because it is the ratio of kinetic rate constants and the initial concentration. As  $d$  increases, the stability of the flow is increased and the number of fingers we see is reduced as the maximum of the growth curve shifts towards the lower wave number. The system becomes more unstable when  $Da$  increases and  $d$  decreases. These results are in qualitative agreement with the trends depicted by the density fingering situation for the same chemical kinetics as observed by De Wit.<sup>11</sup> We conclude that there is significant similarity between viscous fingering and density fingering even though the physical mechanism which generates the instability is different in the two cases.

We now discuss the dispersion curves for the adiabatic system. When the system is operated nonisothermally the dependence of viscosity on both concentration and temperature has to be considered. Heat is released or consumed during the reaction depending on whether the reaction is exothermic or endothermic, respectively. The viscosity dependence now is governed by the coefficients  $R_c$  and  $R_T$ . Since we are interested in liquids flowing through the porous media and the viscosity of liquids decreases with temperature, we restrict ourselves to  $R_T < 0$ . We first discuss the effect of  $Le$  on the dispersion curves for nonisothermal reactions. We see contrasting effects for exothermic and endothermic reactions. In an exothermic reaction, an increase in  $Le$  tends to stabilize the interface, but in the case of an endothermic reaction, an increase in instability is observed for an increase in  $Le$ .  $Le$  greater than 1 implies that the heat conduction is faster than concentration diffusion. When  $Le$

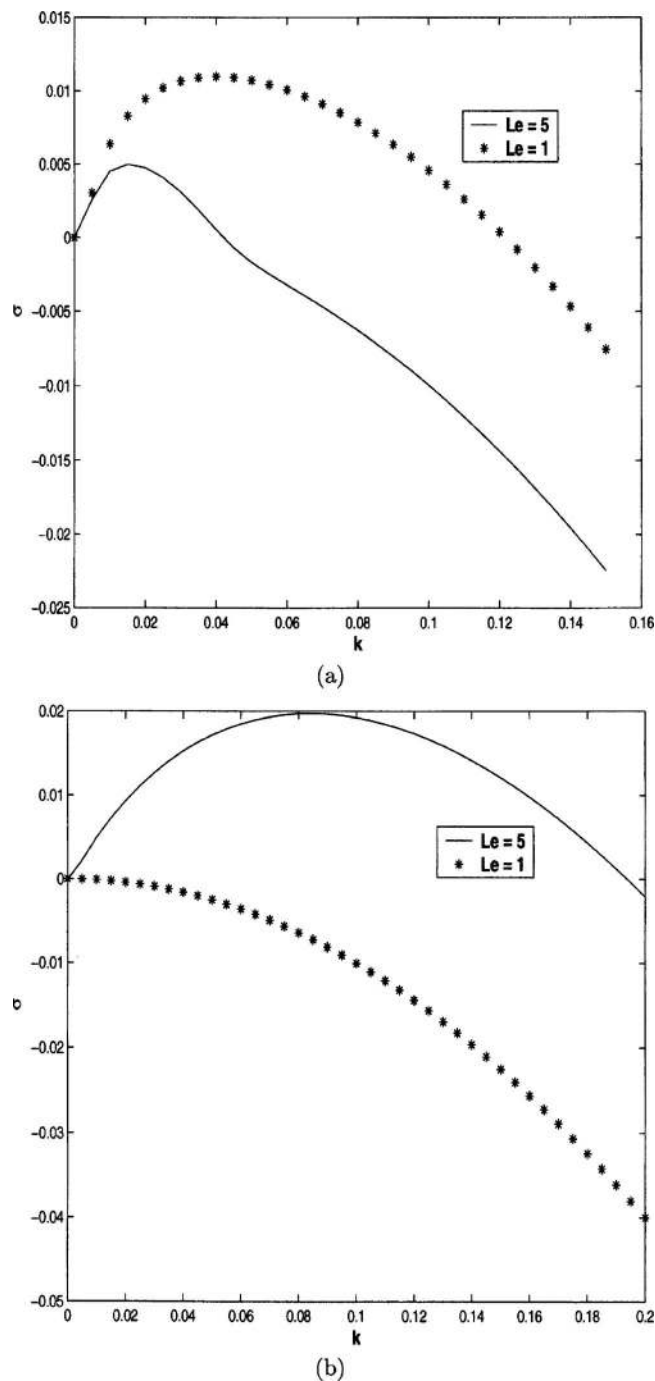


FIG. 4. Dispersion curve showing the variation of growth constant with wave number. (a) Effect of  $Le$  for an exothermic reaction for  $R_c=0$ ,  $R_T=-3$ ,  $Da=0.001$ , and  $d=0.1$ . (b) Effect of  $Le$  for an endothermic reaction for  $R_c=3$ ,  $R_T=-3$ ,  $Da=0.001$ , and  $d=0.1$ .

increases, the temperature gradient that exists in the domain decreases. For an exothermic reaction, because the temperature gradient generates instability in the interface, a decrease in the temperature gradient tends to move the system to a stable regime. Hence, if the temperature is more uniform, the amplitude of the instability is reduced. In an endothermic reaction, the temperature gradient stabilizes the flow. So if the gradient is less the instability is amplified. Figure 4(a) shows the effect of  $Le$  on the dispersion curve for an exothermic reaction, whereas Fig. 4(b) shows the effect for an endothermic reaction.

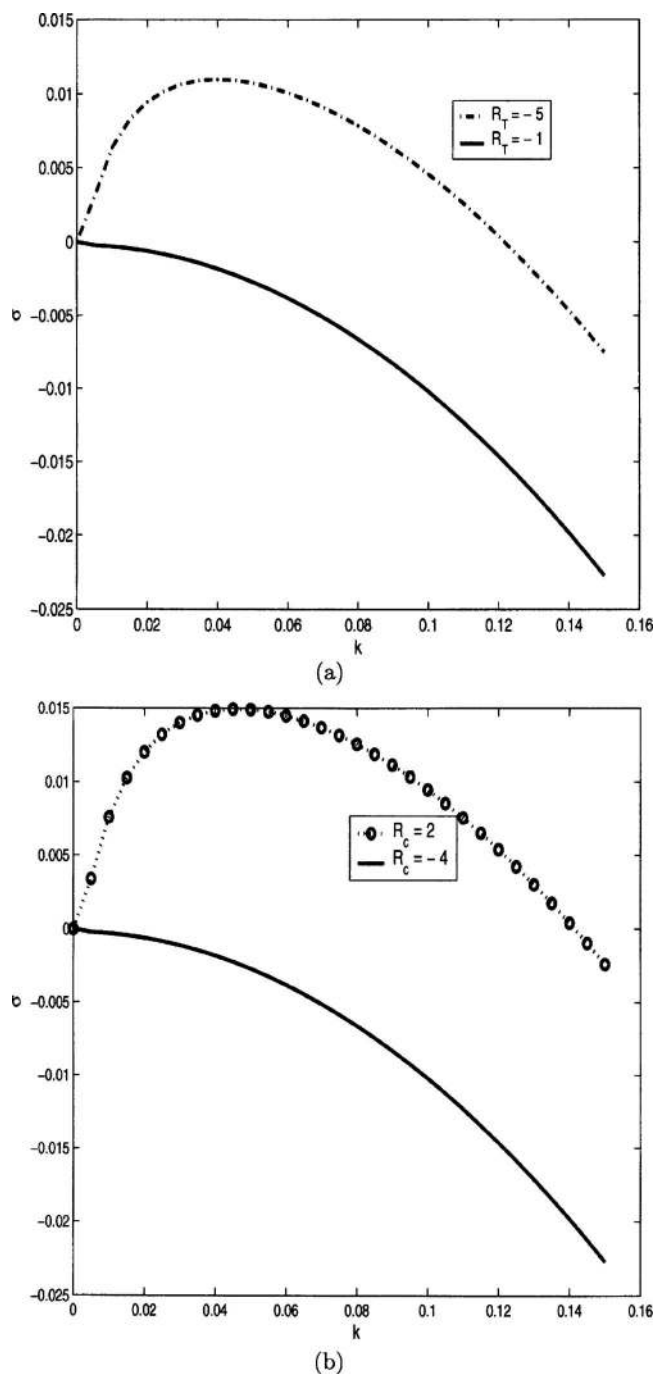


FIG. 5. Dispersion curve showing the variation of growth constant with wave number. (a) Effect of  $R_T$  for an exothermic reaction for  $R_c = -2$ ,  $Le = 1$ ,  $Da = 0.001$ , and  $d = 0.1$  (b) Effect of  $R_c$  for an exothermic reaction for  $R_T = -2$ ,  $Le = 1$ ,  $Da = 0.001$ , and  $d = 0.1$ .

Figure 5 shows the effect of parameters  $R_c$  and  $R_T$  on the stability for an exothermic reaction. If viscosity is considered to be a function of temperature alone ( $R_c = 0$ ), the process again consists of a low viscous fluid invading a high viscous fluid. This generates the viscosity gradient leading to the fingered interface. Incorporation of the temperature dependency on viscosity here makes the flow more unstable. This can be attributed to the fact that the products are at a higher temperature and, hence, a lower viscosity. The products invade the reactants which are at a lower temperature and more viscous. A stronger temperature dependency of viscosity im-

plies  $R_T$  is more negative. The dispersion curve for  $R_T = -5$  lies above that for  $R_T = -1$  which shows this intensification of the instability [Fig. 5(a)]. Figure 5(b) shows the effect of the parameter  $R_c$  on the dispersion curves. Previously, from the isothermal ( $R_T = 0$ ) studies, it has been observed that a negative value of  $R_c$  implies a stable system. However, in the present situation, we have two competing effects as the system is adiabatic. Here neither  $R_c$  nor  $R_T$  is zero. Here we observe that, although we have a destabilization effect due to the temperature dependence of viscosity, the flow gets stabilized for a sufficiently negative value of  $R_c$ . A negative  $R_c$  implies that a high viscous fluid invades a low viscous fluid, while a negative  $R_T$  implies the opposite. Figure 6 shows the effect of  $R_c$  and  $R_T$  on the dispersion curves for an endothermic reaction. Here we find the effect of the parameter  $R_T$  to be the opposite to what was observed for an exothermic reaction. This parameter has a tendency to stabilize the flow. Figure 6(a) shows the effect of  $R_T$  whereas Fig. 6(b) shows the effect of  $R_c$  on the dispersion curves for an endothermic reaction under adiabatic conditions. Heat is consumed during the reaction and, thus, the reactants are at a higher temperature now, and so there is a temperature increase in the flow direction. Under this condition the products are more viscous and a stable front (high viscous fluid invading a low viscous fluid) is observed for a fixed  $R_c$  for sufficiently negative  $R_T$ . The system is on the threshold of stability for  $R_T = -3$  and becomes unstable for sufficiently large positive  $R_c$  only [Fig. 6(b)]. Similarly, for  $R_T = -3$ , the system is on the threshold of instability for  $R_c = 3$ . As  $R_c$  increases the system becomes unstable since now the destabilizing effect of concentration dominates over the stabilizing influence of temperature [Fig. 6(b)]. An adiabatic liquid-liquid reacting system is hence more stable if the reaction is endothermic. From Figs. 5 and 6, we observe that if we fix either  $R_c$  or  $R_T$  (for a fixed set of other parameters) then the value of the other parameter ( $R_T$  or  $R_c$ ) can be estimated at which there is a transition from the unstable to the stable regime. In Fig. 7 we depict the dependence of the critical  $R_c$  on  $R_T$  for two different  $Le$ . For a given  $R_T$ , the critical  $R_c$  represents the value of  $R_c$  across which the instability is induced. Figure 7(a) depicts the boundary for an exothermic reaction. The region above the curve is unstable, whereas the region below the curve is stable. From the figure, we see that the region of stability increases as  $Le$  increases. We see in Fig. 7(a) that a higher viscosity gradient (more negative  $R_c$ ) is required for the flow to become stable. Similarly, for an endothermic reaction,  $Le = 5$  is more unstable [Fig. 7(b)] and, hence, that curve lies below the  $Le = 1$  curve. Here, both  $R_T$  and negative  $R_c$  have a stabilizing influence. The curves are plotted for positive  $R_c$  values which is the region where we observe the transition from stability to instability. Here also, the region lying above the curve is unstable, whereas the region below the curve is stable. For the case when  $Le = 1$ , the stability boundary is  $R_c = R_T$  for an exothermic reaction since the  $T$  and  $c$  profiles are identical for the base traveling wave solution. Similarly,  $R_c = -R_T$  is the stability boundary for an endothermic reaction. Our stability predictions confirm these results. We con-

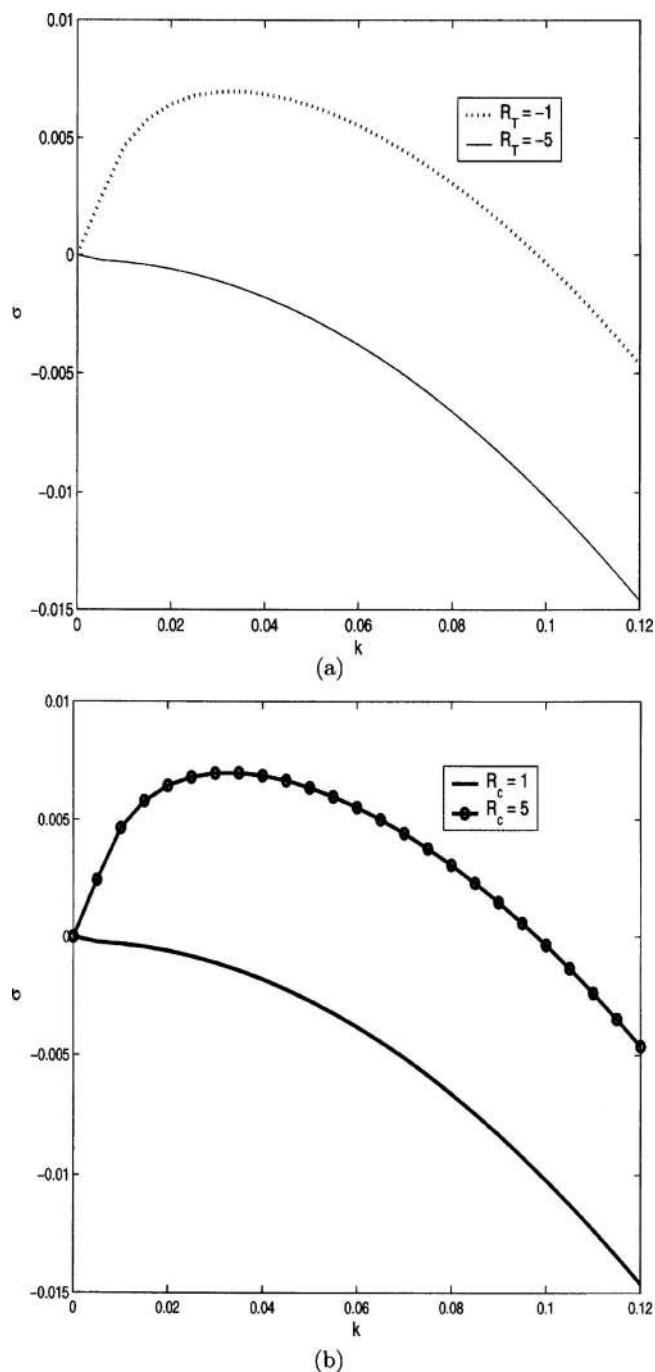


FIG. 6. Dispersion curve showing the variation of growth constant with wave number. (a) Effect of  $R_T$  for an endothermic reaction for  $R_c=3$ ,  $Le=1$ ,  $Da=0.001$ , and  $d=0.1$  (b) Effect of  $R_c$  for an endothermic reaction for  $R_T=-3$ ,  $Le=1$ ,  $Da=0.001$ ,  $d=0.1$ .

clude the section by stating an observation regarding the dispersion curve. These curves do not change significantly once the system is stable.

## V. NONLINEAR SIMULATION

To verify the predictions of the linear stability analysis nonlinear simulations were performed using a finite difference technique. We now describe the algorithm on which the numerical simulation of Eqs. (15)–(18) is based. The spatial discretization of the partial differential Eqs. (15)–(18) is done using a second order central finite difference. Hence,

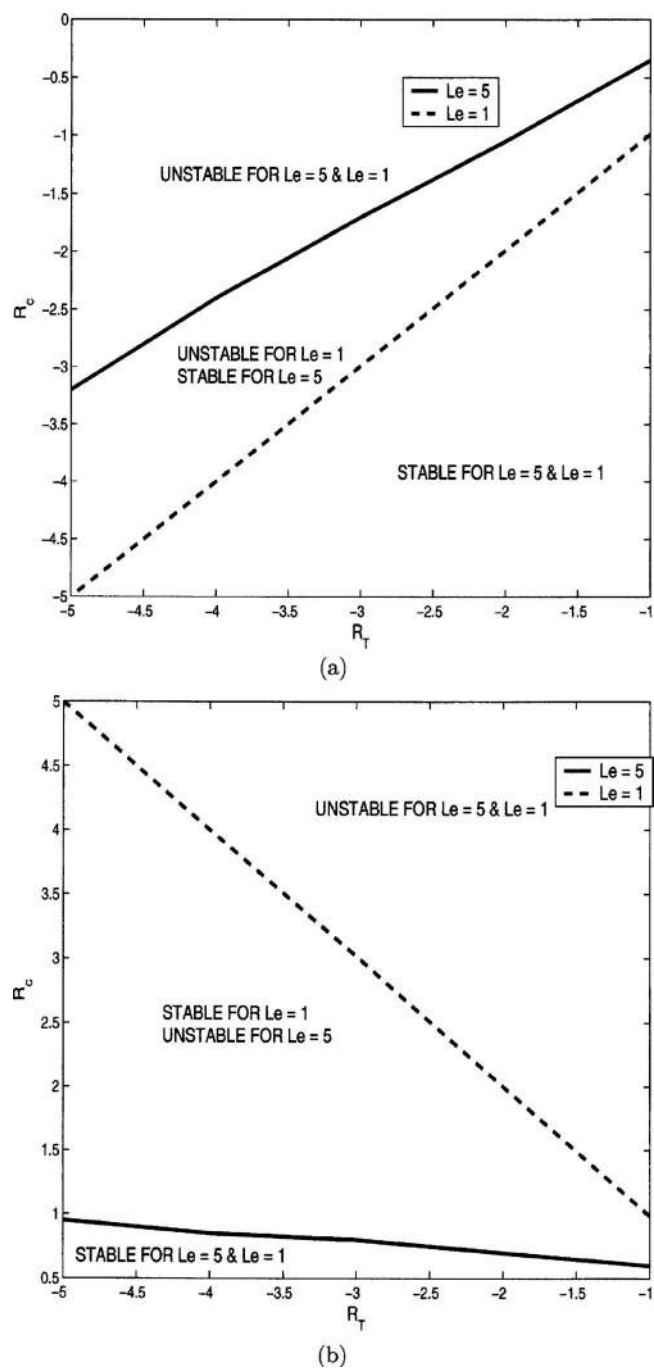


FIG. 7. Critical values in  $R_c$ - $R_T$  plane showing the shift from stability to instability. (a) Exothermic reaction with  $Da=0.001$  and  $d=0.1$ . The region above the solid curve is unstable for both  $Le$  and the region below the dotted curve is stable for both  $Le$ . The region between the two curves is stable for  $Le=5$  but unstable for  $Le=1$ . (b) Endothermic reaction with  $Da=0.001$  and  $d=0.1$ . The region above the dotted curve is unstable for both  $Le$  and the region below the solid curve is stable for both  $Le$ . The region between the two curves is unstable for  $Le=5$  but stable for  $Le=1$ .

the accuracy in space is maintained at  $O(\Delta x^2)$ . The temporal discretization scheme used is a first order forward difference. We use a grid size of 256 (along the  $x$  direction) by 128 (along the  $y$  direction) in most of the simulations. We have also used a larger grid size of  $512 \times 256$  to verify the numerical accuracy and grid independence of the numerical results. The state variables are calculated at each and every node  $(i, j)$ . The algorithm consists of the following steps.

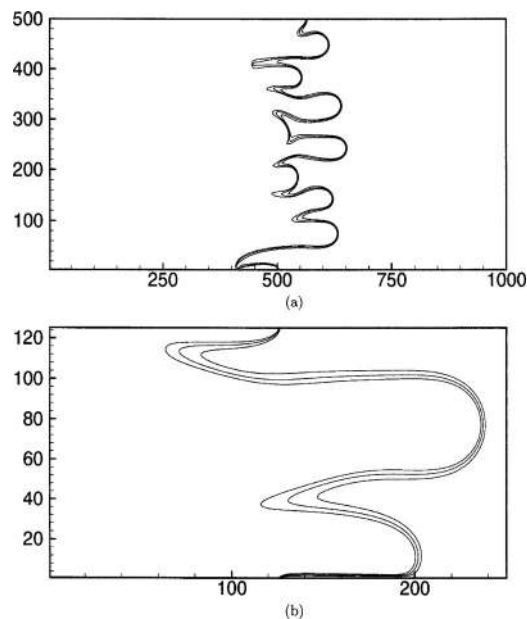


FIG. 8. Nonlinear simulation of an isothermal reaction, the effect of Pe for  $A=2$ ,  $t=200$ ,  $R_c=3$ ,  $Da=0.01$ , and  $d=0.1$ : (a)  $Pe=500$  and (b)  $Pe=125$ .

- Step 1: The convective-diffusion equation [Eq. (17)] is integrated first to calculate the concentration at the new time step  $c(t+\Delta t)$ . This is carried out by using a forward in time central in space scheme. The temperature at the new time step  $T(t+\Delta t)$  is also evaluated in a similar way using Eq. (18).
- Step 2: We use the values of  $c(t+\Delta t)$ ,  $T(t+\Delta t)$ , and  $\psi(t)$  in Eq. (16) to obtain  $\omega(t+\Delta t)$  using a semi-implicit method.
- Step 3:  $\omega(t+\Delta t)$  obtained in the previous step is used for calculating  $\psi(t+\Delta t)$  from Eq. (15). This is iterated using a Gauss-Seidel method for each of the grid points until the values converge.
- Step 4:  $\omega(t+\Delta t)$  is calculated from Eq. (16) using the updated  $\psi(t+\Delta t)$ ,  $c(t+\Delta t)$ , and  $T(t+\Delta t)$ .
- Step 5: This is used in Eq. (15) for refining the estimate of  $\psi(t+\Delta t)$ . In particular, Eqs. (15) and (16) are solved together iteratively until we have convergence. This ensures us that  $\psi$  and  $\omega$  have converged for the present time step.
- Step 6: The estimates of  $c(t+\Delta t)$  and  $T(t+\Delta t)$  are refined using the updated  $\psi$  and  $\omega$ . This confirms the convergence of  $c$  and  $T$  within a time step before we move to the next time step.

In Fig. 8 we depict the effect of Pe on the nonlinear transient behavior for an isothermal reaction. The figures depict the contour plots for the concentration in the range of 0.1–0.3. The total time for the simulation was 50 s. It can be seen that there is a significant effect of Pe on the fingering patterns. For low Pe number ( $Pe=125$ ) the system is well into the nonlinear regime. Here, the fingers are wide and the number of fingers is lower when compared to the higher Pe ( $Pe=500$ ). Peclet number is a measure of the dimensionless

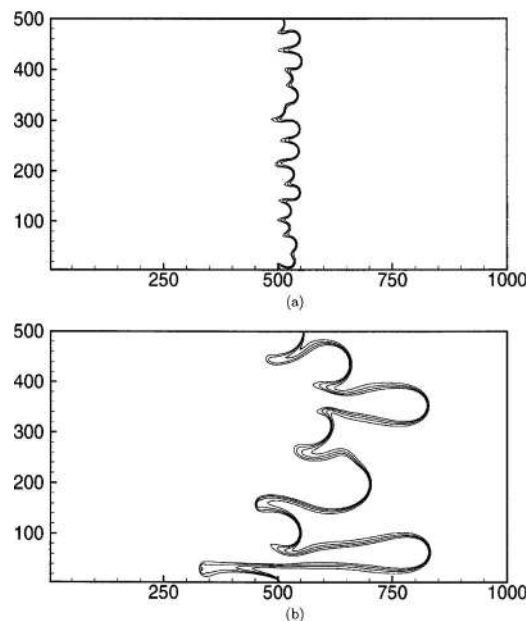


FIG. 9. Nonlinear simulation of an isothermal reaction showing the time evolution profiles for  $Pe=500$ ,  $A=2$ ,  $Da=0.01$ , and  $d=0.1$ : (a)  $t=100$  s and (b)  $t=400$  s.

width of the domain. The aspect ratio is maintained the same for both figures so that length also decreases with a decrease in Pe. So the total time required for the front to reach the end of the domain decreases as Pe is lowered as can be seen in Fig. 8.<sup>7,9</sup> The front has to spread to allow other fingers to grow before it can split. Pe is an important parameter determining this characteristic. Thus, fluid is in the highly nonlinear regime for low Pe because the total time required for reaching the end of the domain is less and, hence, the fingers are more distinct (spreading and shielding<sup>7</sup>). Figure 9 shows how the concentration contours of an unstable system evolves with time. In Fig. 9(a) there are numerous fingers which are very small in size at a time instant of  $t=100$  s. Figure 9(b) is at a later time instant and, hence, the fingers are more pronounced and the number of fingers decreases. There is a fundamental difference of the time evolution profiles in the presence and absence of a reaction. The mean position of the interface is at the same point for a nonreactive system, whereas in the reactive system we see that the average position gets shifted towards the right. As time proceeds the system starts showing nonlinear behavior. The fingers become wide and merge at later time instants, and in the final stages, there are just a few dominant fingers occupying the whole width of the chamber. Figure 10 shows how the viscosity dependency on concentration affects the fingers observed under isothermal flow conditions. For a positive  $R_c$  a low viscous fluid invades a high viscous fluid. Here we observe a fingered structure as in Fig. 10(a). In Fig. 10(b) the front moves as a stable plug. The perturbation to the interface decays in the second case as  $R_c < 0$  and, here, a high viscous fluid flows into a low viscous fluid. The effect of the reaction kinetic parameter  $d$  has also been studied but is not shown here as they show the same trends as discussed previously in the literature<sup>24</sup> (in the vertical configuration).

Nonlinear simulations were also performed for the

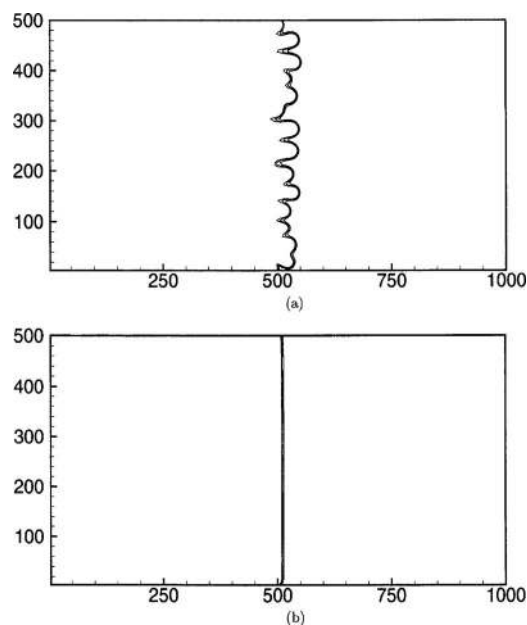


FIG. 10. Nonlinear simulation of an isothermal reaction for studying the effect of  $R_c$  for  $Pe=500$ ,  $A=2$ ,  $t=50$ ,  $Da=0.01$ , and  $d=0.1$ : (a)  $R_c=3$  and (b)  $R_c=-3$ .

nonisothermal system. The parameter values were chosen so that they could confirm the predictions of the linear stability analysis. The parameter  $R_T$  can only attain negative values for liquids. It has a destabilizing effect for an exothermic reaction and a stabilizing effect for an endothermic reaction. The products are at a higher temperature for an exothermic reaction, so a fluid with a lower viscosity displaces one with higher viscosity in an exothermic reaction. The endothermic reaction leads to a condition where the viscosity of the invading fluid is higher than that of the defending fluid and, hence, the flow is stable. This situation prevails in the absence of viscosity being a function of concentration. If the viscosity becomes a function of both concentration and temperature then both dependencies affect the flow stability. Figure 11 depicts the contour plots for an exothermic reaction with  $R_T=-2$ . In Fig. 11(a) the value of  $R_c=2$  and here both the concentration and temperature have a destabilizing influence and we see prominent fingers. When  $R_c=-3$ , the stabilizing influence of concentration dependency dominates the destabilizing influence of temperature dependency and we observe a stable pattern [Fig. 11(b)]. Figure 12 shows the effect of  $R_T$  keeping  $R_c$  at a constant value. A more negative  $R_T$  implies a stronger dependency of viscosity on temperature. For an exothermic reaction the temperature dependency of viscosity results in a destabilizing influence. We see that  $R_T=-5$  shows a fingered interface when compared to  $R_T=-1$  [Fig. 12(b)]. Here the concentration dependency of viscosity stabilizes the flow since it dominates the temperature dependency. Similar studies were conducted on endothermic reactions. Figure 13 shows the effect of the parameter  $R_c$ . An endothermic reaction can exhibit fingers only with a sufficiently high positive  $R_c$  [Fig. 13(a)]. When  $R_c$  is lowered both  $R_c$  and  $R_T$  stabilize the perturbed interface [Fig. 13(b)]. Figure 14 is similar to Fig. 12 but is for adiabatic endothermic reactions. In Fig. 14 we depict contour plots for an en-

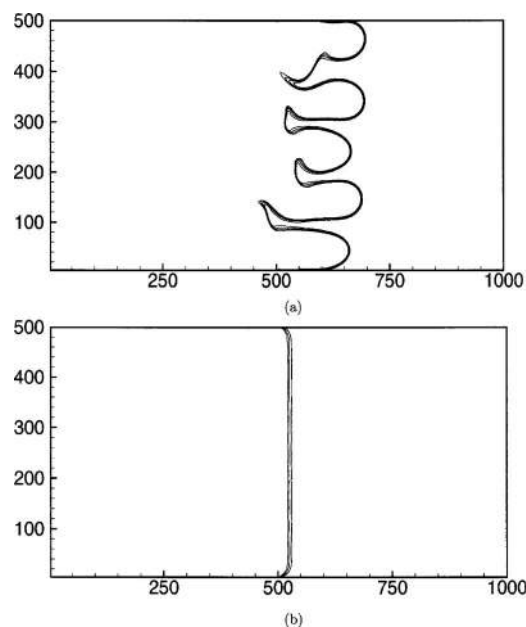


FIG. 11. Nonlinear simulation of an exothermic adiabatic reaction, the effect of  $R_c$  for  $R_T=-2$  and the remaining parameters being fixed at  $Pe=500$ ,  $A=2$ ,  $t=200$ ,  $Le=1$ ,  $Da=0.001$ , and  $d=0.1$ : (a)  $R_c=2$  and (b)  $R_c=-3$ .

dothemic reaction. We see that a more negative value of  $R_T$  stabilizes the flow, whereas an  $R_T$  value which is less negative results in finger formation. This is in accordance with the predictions of linear stability analysis [Fig. 6(a)]. For a fixed  $R_c$  we observe that increasing the value of  $R_T$  (approaching zero) leads to fingerlike structure formation.

In the linear stability analysis, we had observed contradictory effects of  $Le$  for exothermic and endothermic reactions. Figures 15 and 16 confirm this contradictory effect. For an exothermic reaction an increase in  $Le$  leads to a decrease in the temperature and viscosity gradient and, hence, this tends to stabilize the flow. Temperature gradient has a

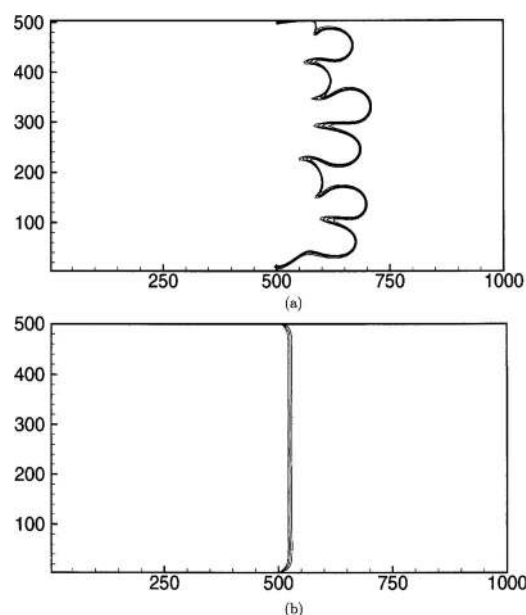


FIG. 12. Nonlinear simulation of an exothermic adiabatic reaction, the effect of  $R_T$  for  $R_c=-2$  and the remaining parameters being fixed at  $Pe=500$ ,  $A=2$ ,  $Le=1$ ,  $t=200$ ,  $Da=0.001$ , and  $d=0.1$ : (a)  $R_T=-5$  and (b)  $R_T=-1$ .

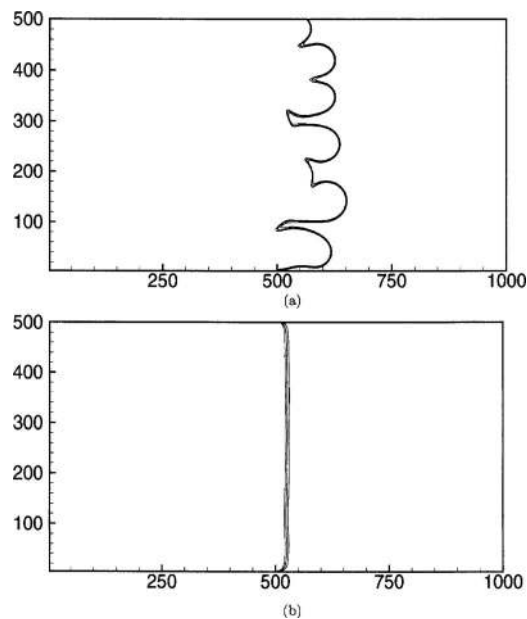


FIG. 13. Nonlinear simulation of an endothermic reaction, the effect of  $R_c$  for  $R_T = -3$ ,  $Pe = 500$ ,  $A = 2$ ,  $t = 200$ ,  $Le = 1$ ,  $Da = 0.001$ , and  $d = 0.1$ : (a)  $R_c = 5$  and (b)  $R_c = 1$ .

destabilization effect on the interface for an exothermic reaction, and, thus, a large  $Le$  implies a reduced temperature gradient and, hence, reduction in the instability (Fig. 15). Increase in  $Le$  on the other hand tends to increase the instability for an endothermic reaction. This is accompanied by an increase in the number of fingers. A large value of  $Le$  implies that the heat diffuses much faster than the concentration. Here, the system tends to move towards the isothermal behavior and the stabilizing influence of temperature gradient is reduced. The stabilization caused by the temperature gradient is absent if the  $Le$  is high. Large  $Le$  endothermic flows are more prone to show instability. For an endothermic reac-

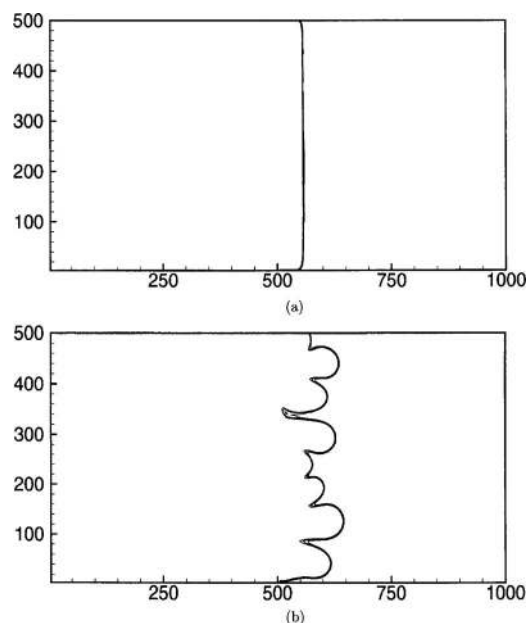


FIG. 14. Nonlinear simulation of an endothermic reaction, the effect of  $R_T$  for  $R_c = 3$ ,  $Pe = 500$ ,  $A = 2$ ,  $t = 200$ ,  $Le = 1$ ,  $Da = 0.001$ , and  $d = 0.1$ : (a)  $R_T = -4$  and (b)  $R_T = -1$ .

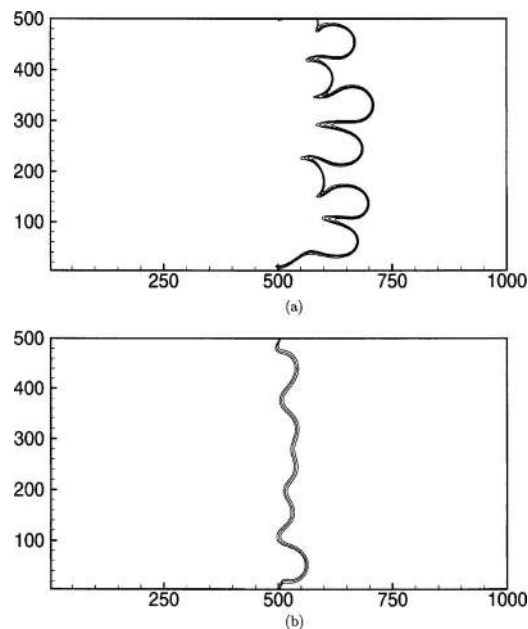


FIG. 15. Nonlinear simulation of an exothermic reaction, the effect of  $Le$  for  $R_c = 0$ ,  $R_T = -3$ ,  $Pe = 500$ ,  $A = 2$ ,  $t = 200$ ,  $Da = 0.001$ , and  $d = 0.1$ : (a)  $Le = 1$  and (b)  $Le = 5$ .

tion, the increase in  $Le$  leads to a decrease in the viscosity gradient and, hence, destabilizes the flow (Fig. 16).

## VI. SUMMARY AND CONCLUSIONS

In this work we have theoretically analyzed an autocatalytic reaction occurring in a fluid flowing horizontally in a porous medium. The kinetic expression of the classical IAA reaction system was chosen for the investigation. We have analyzed the effect of viscosity varying with both tempera-

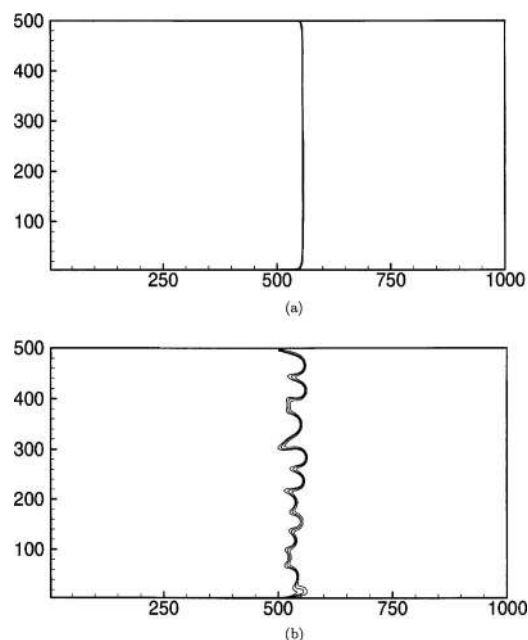


FIG. 16. Nonlinear simulation of an endothermic reaction, the effect of  $Le$  for  $R_c = 3$ ,  $R_T = -4$ ,  $Pe = 500$ ,  $A = 2$ ,  $t = 200$ ,  $Da = 0.001$ , and  $d = 0.1$ : (a)  $Le = 1$  and (b)  $Le = 5$ .

ture and concentration in such systems. Such effects are significant in the area of polymer reaction engineering.

A traveling wave was found as the reference solution and its stability was determined. The stability predictions were confirmed using nonlinear simulations. The simulations were carried out with the complete nonlinear set of equations to predict the long term dynamics. The simulations were carried out for isothermal as well as adiabatic (exothermic and endothermic) conditions. The parameter  $R_c$  has a destabilizing effect when  $R_c > 0$  since this corresponds to the case when a low viscous fluid displaces a high viscous fluid. It was found that  $R_T$ , the parameter defining the temperature dependent component of viscosity, has opposing effects on stability for exothermic and endothermic reactions. We have analyzed only liquid flows and, hence, restrict ourselves to  $R_T < 0$ . In particular, for exothermic (endothermic) reactions, a stronger temperature dependency of viscosity results in destabilization (stabilization) of the flow. The effect of  $Le$  was also opposite for exothermic and endothermic reactions. A higher  $Le$  for endothermic (exothermic) reaction destabilizes (stabilizes) the flow.

The stability boundary was determined in the two-dimensional  $R_c$ - $R_T$  parameter space. This allows us to determine the operating conditions when we have stable displacement and when there is onset of fingering. The boundaries calculated have been verified with the analytically expected values for the case  $Le=1$ .

The primary contribution of this work is to understand that for exothermic reactions the temperature rise can induce

instability in the traveling wave even when the concentration dependency on viscosity is a stabilizing influence ( $R_c < 0$ ).

- <sup>1</sup>G. M. Homsy, *Annu. Rev. Fluid Mech.* **19**, 271 (1987).
- <sup>2</sup>A. E. Scheidegger, *The Physics of Flow Through Porous Media*, 3rd ed. (University of Toronto Press, Toronto, 1974).
- <sup>3</sup>S. Hill, *Chem. Eng. Sci.* **1**, 247 (1952).
- <sup>4</sup>D. W. Peaceman and H. H. Rachford, *SPE J.* **2**, 327 (1962).
- <sup>5</sup>M. A. Christie and D. J. Bond, *SPE Reservoir Eng.* **2**, 514 (1987).
- <sup>6</sup>C. T. Tan and G. M. Homsy, *Phys. Fluids* **29**, 3549 (1986).
- <sup>7</sup>C. T. Tan and G. M. Homsy, *Phys. Fluids* **31**, 1330 (1988).
- <sup>8</sup>A. De Wit and G. M. Homsy, *Phys. Fluids* **11**, 949 (1999).
- <sup>9</sup>A. De Wit and G. M. Homsy, *J. Chem. Phys.* **110**, 8663 (1999).
- <sup>10</sup>A. De Wit, P. D. Kepper, K. Benyaich, G. Dewel, and P. Borckmans, *Chem. Eng. Sci.* **58**, 4823 (2003).
- <sup>11</sup>A. De Wit, *Phys. Rev. Lett.* **87**, 054502 (2001).
- <sup>12</sup>J. D. Murray, *Mathematical Biology* (Springer, Berlin, 1989).
- <sup>13</sup>J. Yang, A. D'Onofrio, S. Kalliadasis, and A. De Wit, *J. Chem. Phys.* **117**, 9395 (2002).
- <sup>14</sup>S. Kalliadasis, J. Yang, and A. De Wit, *Phys. Fluids* **16**, 1395 (2004).
- <sup>15</sup>J. D'Hernoncourt, S. Kalliadasis, and A. De Wit, *J. Chem. Phys.* **123**, 234503 (2005).
- <sup>16</sup>D. Pritchard, *J. Fluid Mech.* **508**, 133 (2004).
- <sup>17</sup>K. E. Holloway and J. R. de Bruyn, *Can. J. Phys.* **83**, 551 (2005).
- <sup>18</sup>K. E. Holloway and J. R. de Bruyn, *Can. J. Phys.* **84**, 273 (2006).
- <sup>19</sup>A. Saul and K. Showalter, *Oscillations and Traveling Waves in Chemical Systems*, edited by R. J. Field and M. Burger (Wiley, New York, 1985).
- <sup>20</sup>I. Epstein and J. Pojman, *An Introduction to Nonlinear Chemical Dynamics* (Oxford University Press, New York, 1998).
- <sup>21</sup>M. R. Carey, S. W. Morris, and P. Kolodner, *Phys. Rev. E* **53**, 6012 (1996).
- <sup>22</sup>R. Dautray and J. L. Lions, *Mathematical Analysis and Numerical Methods for Science and Technology* (Springer-Verlag, Berlin, 1990).
- <sup>23</sup>N. W. Loney, *Applied Mathematical Methods for Chemical Engineers* (CRC, Boca Raton, FL, 2001).
- <sup>24</sup>A. De Wit, *Phys. Fluids* **16**, 163 (2004).